



Effect of filler on thermal aging of composites for next-generation power lines

E. Barjasteh*, N. Kar, S.R. Nutt

1. Department of Chemical Engineering and Materials Science, University of Southern California, Los Angeles, CA 90089, United States

Abstract:

The thermal aging of pultruded composite rods was investigated to determine the effects of filler on oxidation kinetics and degradation mechanisms. The unidirectional hybrid composite rods were comprised of a carbon-fiber core, a glass-fiber shell, and an epoxy matrix filled with clay particles. A reaction-diffusion model was implemented for each of the two hybrid sections to calculate the oxygen-concentration profile and the thickness of the oxidized layer (TOL) within the composite rods, and results were compared with measured oxidation kinetics. The TOL was measured for samples exposed isothermally in air and in vacuum at 200 °C for up to 13,104 h (1.5 year), and the measured values were similar to modeling predictions (within 10%). The domain validity for the reaction-diffusion model was determined from gravimetric experiments (weight-loss measurement), which showed that after prolonged thermal exposure, the degradation mechanism changed from thermal oxidation to thermal degradation. Thermogravimetric analysis (TGA) was performed to determine the thermal degradation and stability of the aged composite. In addition, the effect of thermal aging on glass transition temperature (T_g) and short beam shear (SBS) strength was determined for isothermal exposures at 180 °C and 200 °C.

Key words: A. Carbon fiber; A. Glass fiber; B. Environmental degradation; Thermal degradation

Please cite this article as E. Barjasteh, S. Nutt “**The effect of filler on thermal aging of next-generation power lines**”, Composites A, 42 [12] 1873-1882 (2011)
DOI<<http://dx.doi.org/10.1016/j.compositesa.2011.08.006>>



1. Introduction

New applications of fiber-reinforced polymer composites (FRPCs) are arising in non-traditional sectors of industry, such as civil infrastructure, automotive, and power distribution. For example, composites are being used in place of steel to support high-voltage overhead conductors. In this application, conductive strands of aluminum are wrapped around a solid composite rod comprised of unidirectional carbon and glass fibers in an epoxy matrix [1]. Composite-core conductors such as these are expected to eventually replace conventional steel-reinforced conductors because of the reduced sag at high temperatures, lower weight, higher ampacity, and reduced line losses [2].

Hybrid composites for overhead power lines are manufactured by pultrusion, a continuous process well-suited to the production of long-span composite parts with constant cross section. In this process, fillers and additives traditionally are used to reduce cost when high-volume production is required. Fillers are also used to facilitate pultrusion, especially for long production runs [3], and thus choosing an appropriate filler type and content is critical to achieve viable pultrusion process and to produce parts with suitable mechanical properties. To illustrate, low filler content results in a relatively low viscosity resin, resulting in insufficient shear forces at the profile/die interface. Therefore, a growing layer of resin or “skin” generally builds up at the die interface, resulting in a dimensional decrease in the final part, and eventually occluding the die. On the other hand, high filler content can induce excessive pressure at the die entrance, reducing resin content and diminishing the ultimate mechanical properties [3]. Although the



effects of fillers on the static and dynamic mechanical properties of pultruded composites have been widely reported [4] and [5], filler effects are complex, and fundamental understanding of these effects is incomplete.

Overhead conductors in service are exposed to moderately high temperatures and moisture for decades, and such exposure can adversely affect the mechanical, physical, and chemical-resistance characteristics of composite cores. In particular, at temperatures near the composite T_g , long-term isothermal exposure in air generally results in the degradation of the polymer matrix [6], [7] and [8] and the fiber–matrix interface [9] and [10], although the fibers are generally unaffected. Matrix oxidation initiates at exposed composite surfaces, causing mass loss, shrinkage, embrittlement, and an increase in matrix density [11]. Shrinkage-induced matrix cracks can lead to further oxidation of interior subsurface layers of the matrix [11]. However, in composites, fiber orientations [12] and fiber–matrix interface strength [9] and [10] can significantly influence the extent of damage.

In a previous study [13], the thermal oxidation of similar hybrid composites without filler was investigated for isothermal exposures of 180 °C and 200 °C in air for up to 1 year. A reaction-diffusion model was developed to predict the oxygen concentration profile and the thickness of the oxidized layer (TOL). The oxidation reaction in the reaction-diffusion equation, as shown in Eq. (1), was derived from the standard oxidation mechanism of polymers [14].

$$\frac{\partial[\text{O}_2]}{\partial t} = D \left[\frac{1}{r} \frac{\partial}{\partial r} \left(r \frac{\partial[\text{O}_2]}{\partial r} \right) \right] - 2r_0 \frac{\beta[\text{O}_2]}{1 + \beta[\text{O}_2]} \left[1 - \frac{\beta[\text{O}_2]}{2(1 + \beta[\text{O}_2])} \right] \quad (1)$$



where D is the diffusivity coefficient, r is the radial direction, t is the aging time, r_0 is the maximal oxidation rate in oxygen excess, and β is the reciprocal of the critical oxygen concentration beyond which oxygen excess is reached. The reaction rate parameters, r_0 and β , varied during the exposure due to the consumption of substrate by the oxidation reaction. These variations can potentially lead to invalid predictions of the TOL and the oxygen-concentration profile, both of which are based on the reaction-diffusion model. However, the consumption rate of the specific epoxy resin used in the previous study was assumed to be slow, and hence the reaction-rate parameters were assumed to remain nearly constant during the aging time. Despite these concerns, the model predictions of the TOL of unfilled composites matched the experimentally measured values within 10% [13].

Inorganic fillers have shown different effects on the thermal oxidation of polymer composites. For example, silica is relatively inert and has a negligible effect on the thermal oxidation of epoxy, while $\text{Al}(\text{OH})_3$ can accelerate oxidation [15]. Likewise, the oxidation of high-density polyethylene is inhibited by additions of mica, kaoline, talc, and CaCO_3 , while STC (sericite–tridymite–cristobalite) accelerates matrix oxidation [16]. Consequently, the thermal oxidation of filled composites is affected by filler type and polymer matrix chemistry.

The purpose of the present work was to determine the effect of fillers on the oxidation kinetics and degradation mechanisms of filled composite rods. The oxidation-reaction kinetic parameters were determined by implementing gravimetric experiments, and the reaction-diffusion model described above was applied to predict the TOL and the oxygen-concentration profile. In



addition, the domain of validity of the reaction-diffusion model was examined by performing long-term gravimetric experiments and comparing the measured behavior to the predicted response. Finally, the effects of composite thermal aging on matrix-dominated properties, particularly SBS (short beam shear strength) and T_g , were investigated.

2. Experimental

2.1 Material and conditioning

Unidirectional hybrid composite rods were produced by pultrusion (Composite Technology Corporation, Irvine, CA). The composite rods were comprised of a carbon-fiber (CF) core (6.8-mm outer diameter, ~69% CF volume fraction) surrounded by a glass-fiber (GF) shell (9.3-mm outer diameter and ~64% GF volume fraction). The composite matrix consisted of a cycloaliphatic epoxy formulation (proprietary), an anhydride curing agent, and inorganic filler particles. A commercial-grade kaolinite clay (ASP400p, Huber Engineering Material, Atlanta, GA), which is widely used in pultrusion, was chosen as a filler for use in this study. Filler (12 phr) was mixed with resin and hardener for 15–20 min using a high-shear mixer. In addition, clear castings of neat epoxy and filled epoxy (without fibers) were produced as control samples. The resin mixture was cast in a cylindrical mold and cured at 200 °C for 1 h according to the manufacturer's recommendation. Unidirectional hybrid composite rods, with filler (A) and without filler (B), were cut to lengths of 25.4 mm and sample ends were capped with a silicone sealant to prevent oxygen diffusion through the cut ends and to restrict oxygen diffusion to the radial direction only. (This resembles anticipated service



conditions, in which conductors are strung between lattice towers, and composite ends are encased in metallic fixtures). Prior to exposure, all samples were air-dried at 100 °C for 5 h to remove any retained moisture or low-molecular-weight volatiles. The samples were then placed in an air-circulating oven (for isothermal thermal-oxidation experiments) and in a vacuum oven (for isothermal thermal-degradation experiments) at 180 °C and 200 °C. Samples were removed at intervals and the weight changes were recorded using an analytical balance (ACCULABLA-60) with 0.001 mg accuracy. Prior to weight measurement, each sample was placed in a desiccator for 10–15 min to cool, thus preventing moisture absorption and a change in sample weight.

2.2 Material testing, mechanical testing, and thermal analysis

Oxygen-diffusivity measurements were performed on two types of thin-film clear-cast samples, A and B, using the half-time method [17] (Mocon Company, Minneapolis, MN). Table 1 shows the oxygen diffusivity and solubility values of the composites calculated from the diffusivity data obtained from the bulk using the scaling law ($TOL_c/TOL_b \sim \sqrt{D_c/D_b}$), where D_c and D_b are the diffusivities of composite and bulk, respectively [11]). Note that the radial diffusion coefficient for the filled composites was slightly less than that of the unfilled composite. Henry's equation was used to obtain the oxygen concentration at the surface of the sample, $C_s = S \cdot P_{O_2}$, where S is the solubility and P_{O_2} is the oxygen partial pressure in ambient (lab) air.



Table 1. Values of oxygen diffusivity at 200 °C for two types of the hybrid composites, A and B, where radial diffusivity is represented by D , and C_s and S are the surface concentration of oxygen and oxygen solubility, respectively.

	D glass shell ($10^{-12} \text{ m}^2 \text{ s}^{-1}$)	Solubility ($10^{-4} \text{ mol m}^{-3} \text{ Pa}^{-1}$)	C_s (mol m^{-3})	r_o (10^{-3} s^{-1})	β (l mol^{-1})
A (filled)	1.07	2.70	5.4	8.8	67
B (unfilled)	1.10	3.52	7.1	8.9	75

Short beam shear (SBS) strength was measured to determine the effects of isothermal exposures. The tests were performed at room temperature in accordance with ASTM D4475-02 using a load frame (INSTRON 5567), a bend fixture with a span length six times the rod diameter, and a crosshead displacement rate of 1.3 mm/min.

Dynamic mechanical analysis (DMA) was carried out to determine the change in glass-transition temperature (T_g) after different thermal-oxidation exposures. A commercial DMA instrument (Q800, TA Instruments) was employed using a dual-cantilever-beam clamp. The DMA tests were performed in accordance with ASTM D7028, and a load frequency of 1 Hz and a ramp rate of 5 °C/min were utilized. The T_g value was determined from the peak in the loss-modulus curve for each composite rod sample. Each reported T_g value was the average of three measured values with a standard deviation of less than 2 °C. Note that the mechanical and thermal properties of as-produced filled and unfilled rods were nearly identical.

Thermogravimetric analysis (TGA; TA Instruments Q5000) was employed to determine the matrix degradation with increasing aging times. Approximately 25 mg of CF core was heated in an open Please cite this article as E. Barjasteh, S. Nutt “**The effect of filler on thermal aging of next-generation power lines**”, Composites A, 42 [12] 1873-1882 (2011)
DOI<<http://dx.doi.org/10.1016/j.compositesa.2011.08.006>>



platinum pan in nitrogen (50 mL/min). A ramp rate of 3 °C/min was employed over a temperature range of 30–700 °C.

The thickness of the oxidized layer (TOL) was measured at different oxidation exposure times by microscopic examination of polished sections. Transverse sections of oxidized samples were cut and polished using a broad-beam ion polisher (JEOL SM-09010). Ion polishing (Voltage: ~5.2 kV and Current: ~110 mA) resulted in sections free of relief, ~1 mm × 1 mm, preserving the delicate oxidized layer. Optical microscopy (DIC microscope 2 (Olympus Vanox)) and scanning electron microscopy (SEM; JSM 7001F Low-Vacuum Field Emission Instrument) were used to examine the polished sections.

2.3 Modeling

A reaction-diffusion model was employed to determine the oxygen concentration and the thickness of oxidized layer within the unidirectional hybrid composites with a particulate-filled matrix. The detailed explanation of the developed model has been presented previously [13]. The oxygen-transport properties and oxidation-reaction-rate parameters were determined for the CF core and the GF shell, then two coupled reaction-diffusion equations, (Eqs. (2) and (3)), were solved numerically using commercial software (MATLAB, MathWorks, Natick, MA).

$$\frac{\partial C_g}{\partial t} = D_{Glass/epoxy} \left(\frac{\partial^2 C_g}{\partial r^2} + \frac{1}{r} \frac{\partial C_g}{\partial r} \right) - r_2(C_g) \quad (2)$$

$$\frac{\partial C_c}{\partial t} = D_{carbon/epoxy} \left(\frac{\partial^2 C_c}{\partial r^2} + \frac{1}{r} \frac{\partial C_c}{\partial r} \right) - r_1(C_c) \quad (3)$$



Here, $D_{glass/epoxy}$ and $D_{Carbon/epoxy}$ are the diffusivities of oxygen through the glass shell and the carbon core, respectively, and $r_2(C_g)$ and $r_1(C_c)$ are the reaction rates of oxygen within the glass shell and the carbon core, respectively. Note that the reaction-rate parameters of the epoxy matrix within the GF shell differed from those of the matrix within the CF core. This reflects the possibility that carbon fibers, unlike glass fibers, could participate in reactions [13].

3. Results and discussion

3.1 Model-based prediction of TOL

Weight-loss measurements were performed to obtain the oxidation-reaction-rate parameters for a filled epoxy sample. Fig. 1 shows weight-loss data for thin-film (30 μm), clear-cast, filled-epoxy samples as a function of aging time at different partial pressures of oxygen (1 atm. total pressure) at 200 °C. The weight-loss rate increased with increasing oxygen partial pressure, indicating that weight loss was directly proportional to the extent of thermal oxidation. Weight loss for samples in a vacuum oven, although slight, clearly indicated that the polymer network was not stable and thermal degradation occurred during the exposure. The weight-loss data of the unfilled epoxy sample exposed at 200 °C in an air-circulated oven is also shown in Fig. 1. The weight-loss rates of the unfilled and filled samples were nearly identical during the exposure (the two dotted lines in Fig. 1) in air, indicating similar oxidation kinetics. The weight-loss rates of filled and unfilled epoxy samples were nearly identical for exposures in vacuum and in pure oxygen.

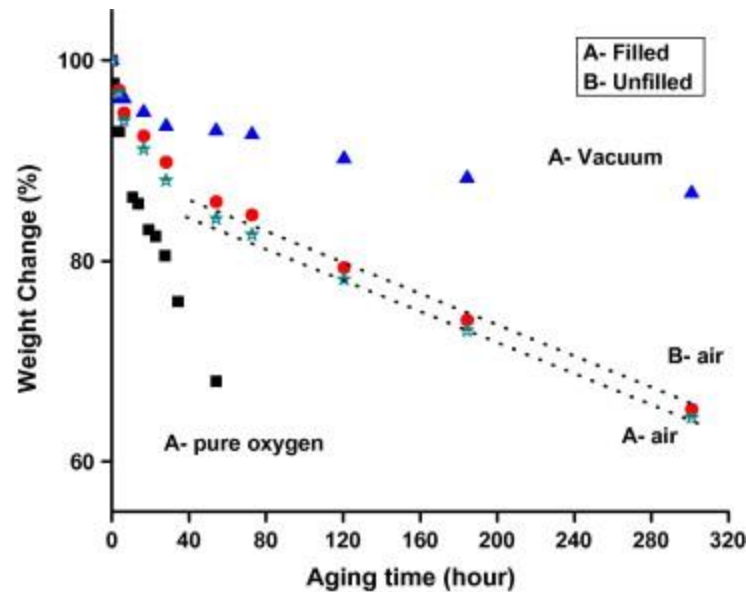


Fig. 1. Weight loss of clay-filled epoxy film samples ($30 \pm 5 \mu\text{m}$ thick) exposed to different partial pressures of oxygen at $200 \text{ }^\circ\text{C}$. The weight loss of filled and unfilled films exposed to air at $200 \text{ }^\circ\text{C}$ is also presented. (For interpretation of the references to color in this figure legend, the reader is referred to the web version of this article.)

Table 1 shows the oxidation reaction-rate parameters, r_o and β , obtained using the weight-loss rates shown in Fig. 1, for the filled and unfilled samples at $200 \text{ }^\circ\text{C}$. The values of the parameters for the filled sample were nearly identical to those for unfilled sample, and the negligible differences were within experimental errors. The results indicate that the clay fillers were inert during hot oxidation in air, and hence did not affect the thermal-oxidation mechanism.

The oxygen-concentration profile, $C(r, t)$, within the composite samples was predicted by numerically solving the two coupled differential equations (Eqs. (2) and (3)) describing the CF core and the GF shell. Fig. 2 shows the calculated oxygen-concentration profiles as a function of radial position for exposure times up to 672 h at $200 \text{ }^\circ\text{C}$. The profiles show that the oxygen concentration decreases and approaches zero with increasing depth in the GF shell for any aging time, and oxygen



never reaches the CF core. Similar oxygen-concentration profiles were predicted for an aging time of 100 h.

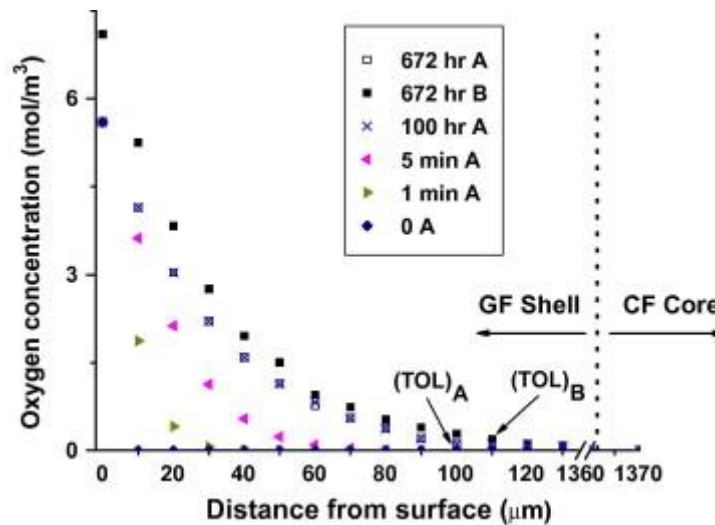


Fig. 2. Calculated oxygen concentration profiles for filled hybrid composite rods (A), $C_c(r, t)$ and $C_g(r, t)$, in air at 200 °C, along with the oxygen concentration profile of the unfilled rod (B) aged for 672 h in 200 °C air. (For interpretation of the references to color in this figure legend, the reader is referred to the web version of this article.)

Fig. 2 also shows the calculated oxygen-concentration profile for an unfilled rod after 672 h exposure (labeled B). The oxygen concentrations of the unfilled rod were slightly greater than those of the filled rods at all depths below the surface, although the profile exhibits the same trend shown by filled rods. The slightly higher oxygen concentrations predicted for the unfilled rods were attributed to the slight increase in oxygen surface concentration and oxygen diffusivity of the unfilled sample. The surface oxygen concentration of the filled rod (5.4 mol m^{-3} , calculated from Henry's law) was less than that of the unfilled rod (7.1 mol m^{-3}) because of the lower solubility of oxygen within the filled sample, as shown in Table 1. Furthermore, because of the longer, more tortuous path for



oxygen diffusion within the filled sample, the oxygen diffusivity (D) was slightly less for the filled material.

The thickness of the oxidized layer can be predicted from the oxidation-product distribution data [13], either via a time integration of reaction rate at radial positions within the sample, or directly from the oxygen-concentration distribution data. In the present case, TOL was taken to be the point at which the oxygen concentration value was nearly zero. As shown in Fig. 2, the TOL values predicted for the filled and unfilled composite samples were 100 and 110 μm , respectively. Note that the TOL values predicted using the oxidation-product distribution data, as explained in [13], were identical to those calculated from the profile of oxygen concentration (TOL = 100 μm).

3.2 Experimental measurements of TOL

To validate the model-based predictions presented above, the thickness of the oxidized layer was measured after oxidizing rods (30.5 mm long) in an air-circulated oven at 180 °C and 200 °C. Sections of the thermally oxidized rods were subsequently ion-polished and inspected to measure the TOL, as shown in Fig. 3a and b. Fig. 3a shows the morphology of the oxidized layer, including matrix cracking and fiber–matrix debonding. However, contrast between oxidized and non-oxidized regions were not suitable for TOL measurement. Light microscope images provided great contrast between oxidized and non-oxidized matrix, as shown in Fig. 3b. The oxidized matrix appears lighter, and gradually become darker by increasing the depth from the surface. Note that the void content did not change after oxidizing the rods.

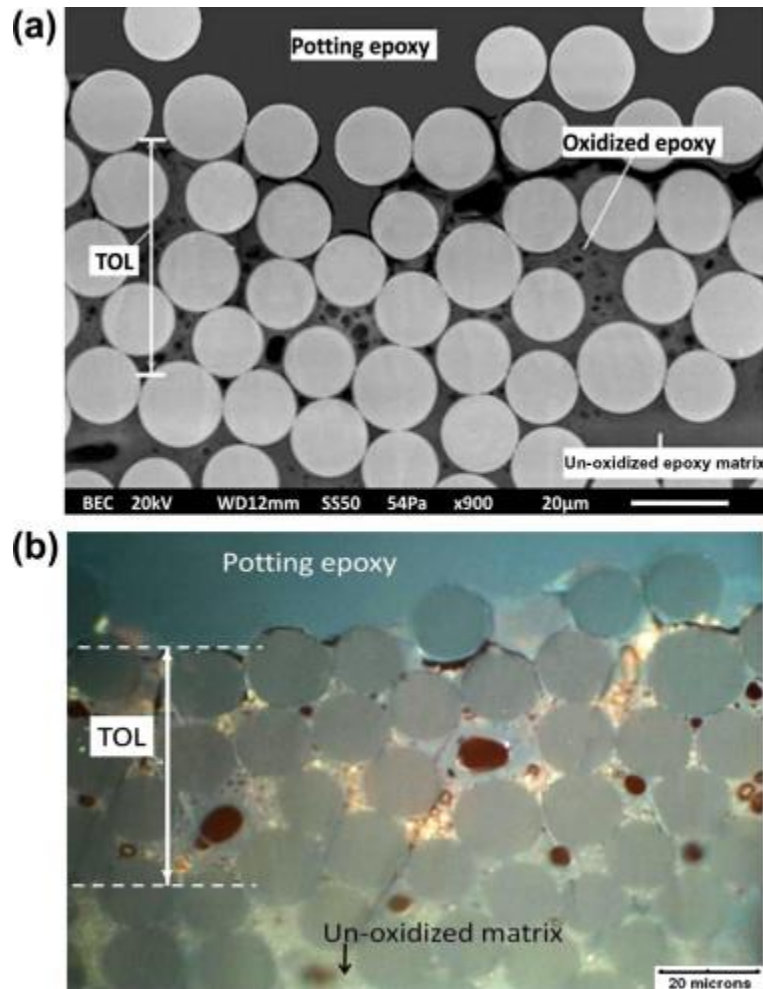


Fig. 3. Transverse cross sections of hybrid composite rods thermally aged in air at 200 °C for 8,736 h taken by (a) SEM (b) optical microscopy. (For interpretation of the references to color in this figure legend, the reader is referred to the web version of this article.)

Table 2 shows the TOL of the filled and unfilled composite rods aged for 672 h at 200 °C, along with the model-based predicted values. The thickness values were determined from an average of over 20 measurements. Differences of roughly 8% and 6% were noted between the measured and predicted TOL values for the filled and unfilled samples, respectively. Note that the oxidation thickness was limited to a superficial layer, and no evidence of oxidation was detected at the interface

between CF and GF regions or within CF core. In addition, the measured TOL showed a decrease

Please cite this article as E. Barjasteh, S. Nutt “**The effect of filler on thermal aging of next-generation power lines**”, Composites A, 42 [12] 1873-1882 (2011)

DOI<<http://dx.doi.org/10.1016/j.compositesa.2011.08.006>>



of $\sim 8 \mu\text{m}$ when inorganic filler was incorporated in the matrix, and a similar decrease in TOL ($\sim 10 \mu\text{m}$) was obtained from the model prediction, as shown in Table 2.

Table 2. Comparison of experimental measurement of TOL with model-based predicted values in air exposed for 672 h at 200 °C for filled and unfilled composite samples.

Temperature (200 °C)	Oxidation	Thickness (TOL)
Sample type	Model prediction (μm)	Experimental measurement (μm)
Filled A	100	109 ± 7
Unfilled B	110	117 ± 5

3.3 Model extension and validity domain

Table 3 shows model-based values of the TOL calculated for filled rods at 200 °C, extended up to 13,104 h (78 weeks or 1.5 year), and measured TOL values are included for comparison. The TOL values calculated from the reaction-diffusion model were 100 μm for all exposure times up to 13,104 h. Transverse sections of the composite samples aged for 13,104 h (78 weeks) at 200 °C and un-aged samples are shown in Fig. 4a and b, respectively. The sections showed no significant changes in the TOL values (within 95–109 μm), even after 78 weeks. Slight variations of the TOL (often decreases) were attributed to superficial surface erosion of the oxidized epoxy matrix (10–20 μm), noted during inspection of aged composite rods. The calculated and measured TOL values differed by roughly 10%, as shown in Table 3. Similar agreement was reported for unfilled rods



[13]. The slight discoloration evident in the oxidized sample was attributed to thermal degradation, discussed in Section 3.4.

Table 3. Experimental measurements and model-based predictions of TOL values for the rods aged at 200 °C in air for several exposure times from 4–78 weeks (13,104 h).

Aging time (weeks)	0	4	36	52	78
TOL (μm) measured	0	109 ± 7	101 ± 11	105 ± 10	95 ± 14
TOL (μm) calculated	0	100	100	100	100

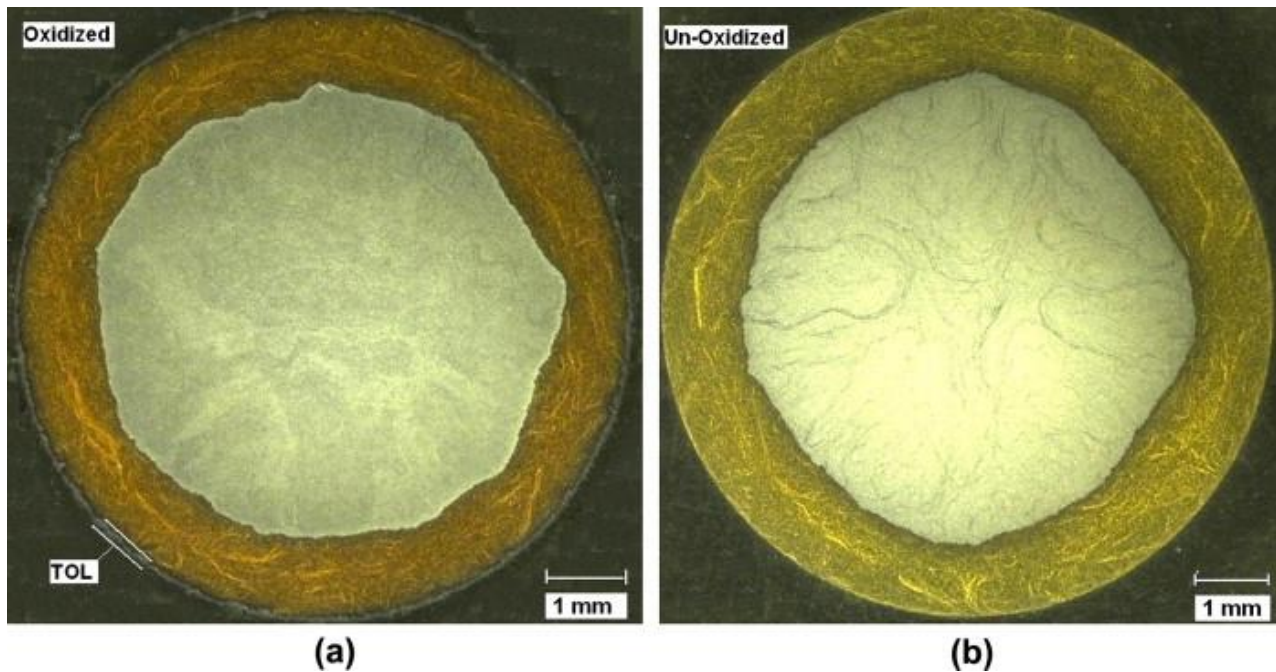


Fig. 4. Transverse cross section of composite rods (a) exposed in 200 °C air-circulated oven for 13,104 h and (b) un-aged. (For interpretation of the references to color in this figure legend, the reader is referred to the web version of this article.)



The accuracy of the reaction-diffusion model predictions of the oxygen-concentration profile depends on the accuracy of the assumptions during exposure. These assumptions refer mainly to the variations of phenomenological parameters (diffusion coefficient, D , and reaction-rate parameters, β and r_o) in the domain of study. For example, the diffusion coefficient changes over time as the epoxy matrix undergoes oxidation. Furthermore, the formation of cracks or other damage to the oxidized surface opens pathways for accelerated penetration of oxygen, and thus the local diffusivity in the vicinity of the crack is effectively increased. The reaction-rate parameters also change during oxidation because of the dependency on the pre-oxidized oxygen concentration. During oxidation, the active sites available to react with oxygen are gradually exhausted during long-term exposures, resulting in a decrease in the oxidation-reaction rate. Consequently, the phenomenological parameters gradually change with time, reducing the model accuracy. However, for the conditions studied here, the weight-loss data was approximately linear for long exposures (up to $\sim 5,000$ h, shown on Fig. 5), implying a slow conversion rate of epoxy and nearly constant model parameters over the relevant exposure times.

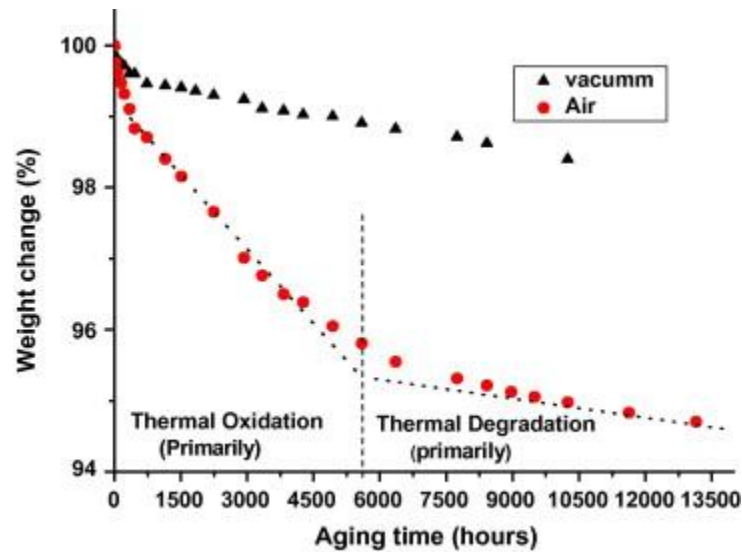


Fig. 5. The weight change of composite rods exposed in 200 °C vacuum and air-circulated ovens for 13,104 h of exposure. (For interpretation of the references to color in this figure legend, the reader is referred to the web version of this article.)

Fig. 5 shows the weight change for filled composite rods aged at 200 °C in air and in vacuum for up to 13,104 h. The weight loss rate was greater in air than in vacuum. The initial weight-loss rate for rods aged in vacuum was high during the first 20–40 h, then decreased to a constant value for the duration of the exposure. The high initial weight-loss rate was attributed to the initial presence of moisture within the sample and to low-molecular-weight volatiles generated from the post-curing reaction. The semi-steady-state weight loss was attributed to thermal degradation of the epoxy matrix due to chain scission and emission of small molecules that commonly occurs during high-temperature exposures (temperatures approaching T_g) [18].

In contrast, the rods aged in air showed a high initial weight-loss rate followed by a secondary weight-loss rate up to 5,500 h. This was followed by a semi-steady condition for the remainder of the exposure, during which the rate was nearly the same as the rods aged in vacuum. The secondary



weight loss of the rods exposed in air was attributed to the emission of low-molecular-weight species such as CO₂, H₂O, and CO during oxidation [6] and [18]. Hence, the primary weight-loss mechanism was identified as thermal oxidation. Thermal degradation (occurring primarily in the bulk of the composite rods) occurred simultaneously, but had a negligible effect on the weight loss during the secondary aging period. The similarity of semi-steady-state weight-loss rates for rods aged in air and in vacuum implies that similar degradation mechanisms were involved for that period of exposure. Thus, aging after roughly 5,500 h in air was attributed primarily to thermal degradation.

The change in the primary matrix-degradation mechanism from thermal oxidation to thermal degradation with increasing aging time corresponded to a change in the oxygen diffusivity, and hence the reaction-diffusion equations. The diffusivity of oxygen within the oxidized epoxy layer gradually changed during the aging period. Unfortunately, direct measurements of diffusivity over time were difficult because of the progressive embrittlement of the oxidized epoxy [13]. However, measurements of elastic modulus provided insight into the extent of the oxygen diffusion. Fig. 6 shows the change in elastic modulus within the TOL region for a bulk epoxy sample oxidized [13]. The elastic modulus within the oxidized layer reached a maximum at the surface (nearly 3× the value of the un-aged epoxy), and decreased with increasing depth beneath the surface, reaching a constant value ~125 m from the surface. (The increase in modulus for the bulk sample aged in *vacuum* was attributed to a post-curing reaction, which increased the crosslink density.) Matrix shrinkage occurred within the TOL, accompanied by an increase in molecular packing density, resulting in the measured increase in elastic modulus, and a decrease in diffusivity. The diffusivity of oxygen within the composite rods decreased over time and became nearly zero after 5500 h (see Fig. 5). The latter



represents a transition point at which the degradation mechanism changes, after which the weight loss rate of rods in vacuum and in air ovens became nearly identical.

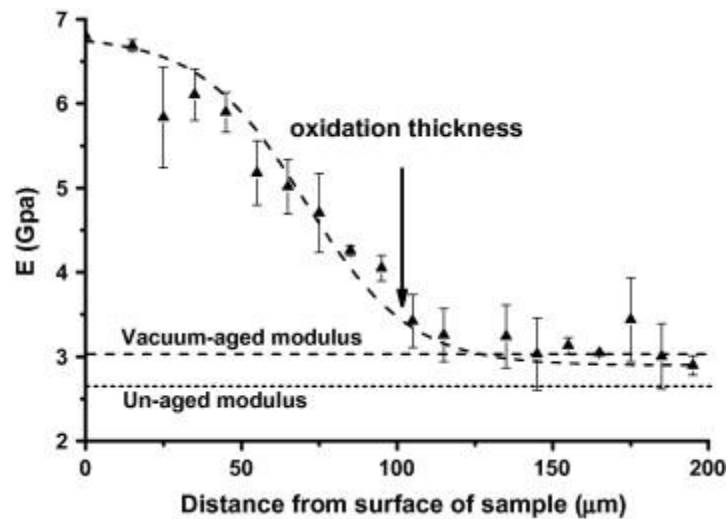


Fig. 6. Elastic modulus as a function of depth for a clear cast polymer sample (3 mm thick) aged for 3200 h at 200 °C [13].

The oxidation reaction in the reaction-diffusion system depended on oxygen availability. After the transition exposure time (~5500 h), the oxidation reaction-diffusion system changed to a simple degradation reaction, and oxygen diffusivity became negligible. Fig. 7 shows the standard closed-loop mechanistic scheme for oxidation of the rods, along with the radical degradation mechanism [14]. The initiation and propagation steps of the thermal-degradation mechanism resulted in emission of volatiles and hence weight loss. Note that the lowest weight-loss rate observed in Fig. 5 (low slope) was for vacuum aging and for air aging beyond 5500 h, indicating a low rate of degradation reactions for these conditions. During radical degradation, the radicals, P° , undergo either chain scission (β scission), as shown in the propagation step in Fig. 7, or radical coupling



(crosslinking), as shown in the termination step. The relation of weight loss rate and kinetic equations can be derived using a radical degradation scheme (beyond the present scope).

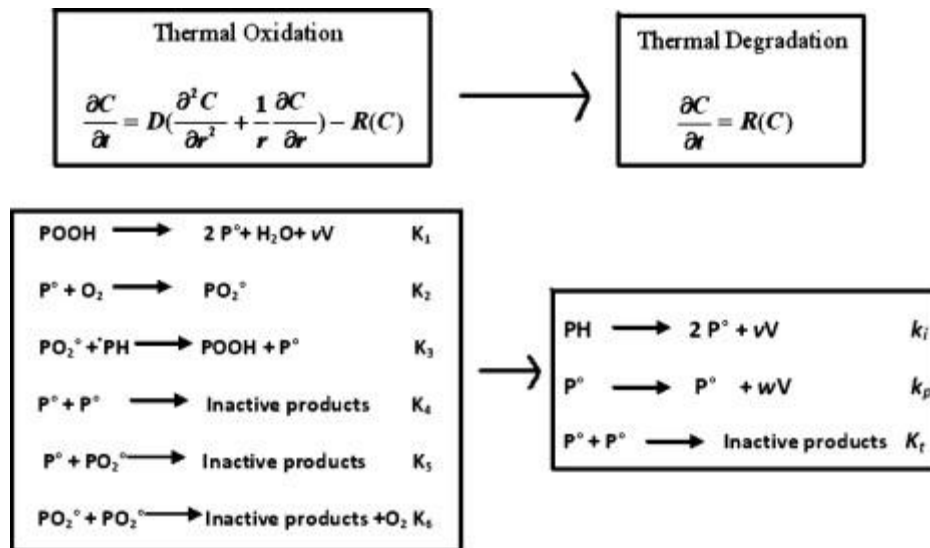


Fig. 7. Closed-loop standard mechanistic scheme for thermal oxidation (left) and radical thermal degradation mechanism (right).

The assumption of a low conversion rate for the composite matrix was valid during thermal oxidation, but not during thermal degradation. Therefore, the reaction-diffusion model used to calculate the oxidized thickness (TOL) was applied only up to the transition exposure time (5500 h). After the transition point, the oxidation rate was negligible, and thermal degradation of the matrix became the primary degradation mechanism. Effectively, the oxidized layer that formed during the early stage of aging protected the bulk of the matrix from further oxidation. This protective effect was facilitated by the alignment of fibers, which inhibited crack formation and propagation.



3.4 Damage

Filled-composite samples were inspected for cracking and damage after thermal aging. Fig. 8 shows the un-aged filled composite rod (left), the thermally aged rod (center), and the hybrid composite coupon (right) exposed for 13,104 h at 200 °C. No matrix cracking or fiber–matrix debonding was observed within the un-aged as-produced rods, indicating no process-induced damage occurred. The composite coupons were sectioned from the rod center to produce beam samples ~1.6 mm thick (the same samples were used for DMA measurements of T_g). With increasing exposure time, the surface changed from yellow (initial) to dark brown, and the discoloration was attributed to surface oxidation. Subsequent discoloration of the bulk rod was attributed to changes in the chemical structure of the epoxy (thermolysis). Note that the cross-section in Fig. 4a also shows matrix discoloration after 1.5 year of aging, caused by changes in the chemical structure of the matrix associated with thermal degradation. In addition, shrinkage of the oxidized matrix resulted in fiber–matrix debonding and exfoliation of 1–2 near-surface fibers, as shown in Fig. 8 (center). Similar results were reported for unfilled rods [13]. Furthermore, the matrix near the surface became embrittled and underwent superficial surface erosion, which was attributed to the internal force induced by matrix shrinkage. In contrast, the oxidation of the composite coupon, as shown in Fig. 8 (right), exhibited a brush-like appearance because of partial detachment of fibers. The apparent width of the coupon increased to ~14.5 mm (initial width was 9.525 mm).

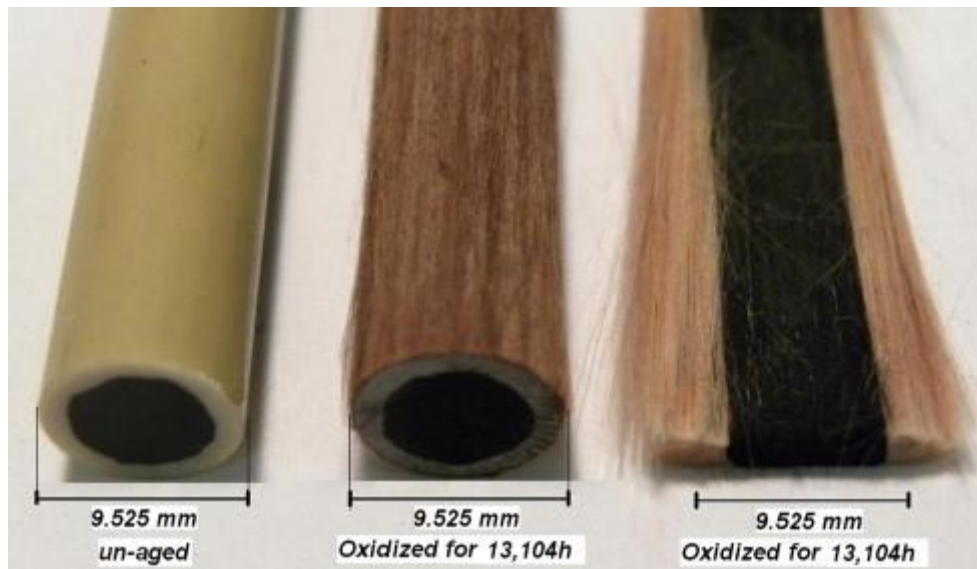


Fig. 8. The transverse cross section of un-aged filled composite rod (left), thermally aged rod (middle), and hybrid composite coupon (right) exposed for 13,104 h at 200 °C. (For interpretation of the references to color in this figure legend, the reader is referred to the web version of this article.)

The evolution of cracks and other oxidation-induced damage was influenced by the sample geometry and fiber orientations at the air-exposed surface. The exceptional damage resistance of composite rods after long-term exposures at 200 °C was attributed in part to the orientation of glass fibers parallel to the exposed surface, and the absence of fibers oriented normal to the surface, which typically provides pathways for accelerated diffusion. Thus, the sample geometry and fiber orientation effectively inhibited surface crack initiation and retarded the advancement of the oxidized layer. Note that coupon samples sectioned from the rod exhibited more severe oxidation damage and fiber exfoliation (Fig. 8), largely because of the two exposed surfaces in close proximity.

Fig. 9 shows transverse sections of (a) filled and (b) unfilled composite rods exposed in air for 8736 h. The sections show the presence of voids near the sample surface. No surface cracks were detected in filled rods oxidized for 1 year, while cracks were observed within a portion of the



oxidized layer (limited to the first 50 μm of the TOL) of unfilled rods, as shown in Fig. 9b. In unfilled rods, cracks initiated from the surface, propagated through the matrix and along fiber/matrix interfaces, and extended to a depth of ~ 50 m. In contrast, the absence of cracks in filled rods was attributed to the increased fracture toughness of the matrix, even at temperatures near T_g [19], [20] and [21]. Filler particles, even at low loadings, reportedly inhibit crack initiation and cause crack deflection and blunting, enhancing toughness [19], [20] and [21]. The cracks in unfilled rods were limited to a thin surface layer (<50 μm), even after 1.5 years exposure at 200 $^{\circ}\text{C}$.

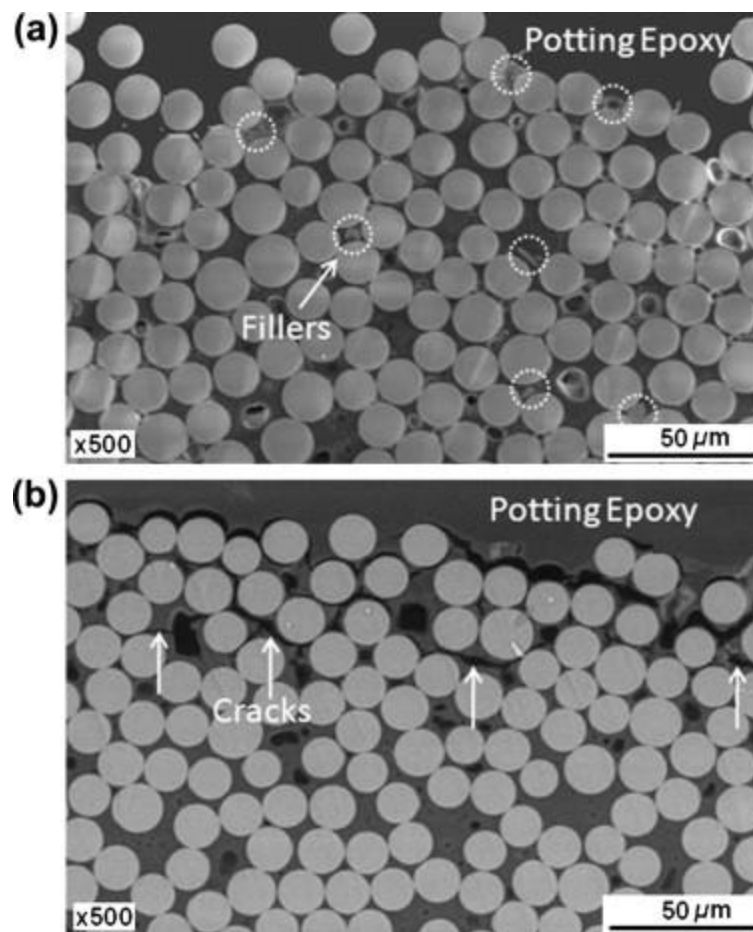




Fig. 9. Transverse cross-section of (a) filled and (b) unfilled composite rods exposed in air for 8,736 h at 200 °C.

3.5 Matrix degradation

Fig. 10 shows the weight change of thermally aged composite rods as a function of temperature up to 700 °C. Composite rods were aged in 200 °C air for 0, 4, 36, and 52 weeks, then test samples were sectioned from CF core regions (removing the oxidized surface) of the aged rods to prepare samples for TGA. Note that the fibers were stable within the temperature range of the TGA experiments. The TGA data indicates that the longer isothermal aging times resulted in higher onset temperatures for weight loss. To illustrate, T_5 , the temperature at which 5% weight loss was reached, is shown in Eq. (4) for several aged rods. After 52 weeks of aging, the degradation-onset temperature increased 21 °C.

$$T_{5,0} [= 330 \text{ °C}] < T_{5,4\text{wks}} [= 331 \text{ °C}] < T_{5,36\text{wks}} [= 343 \text{ °C}] < T_{5,52\text{wks}} [= 351 \text{ °C}] \quad (4)$$

At temperatures above 450 °C, longer isothermal aging times showed less weight loss. For example, the percentages of weight loss for the un-aged rods and rods aged 52 weeks at 500 °C were ~21% and 19%, respectively. The 2% decrease in weight loss after aging can be attributed to the formation of a stable char and other thermo-stable compounds during isothermal aging. The results, together with the mass loss observed during vacuum aging, indicate that the epoxy matrix underwent thermal degradation during isothermal exposure. Note that the weight change as measured by TGA of the rods pre-aged at 180 °C was negligible, even after 52 weeks of exposure, indicating that the matrix was thermally stable at 180 °C.

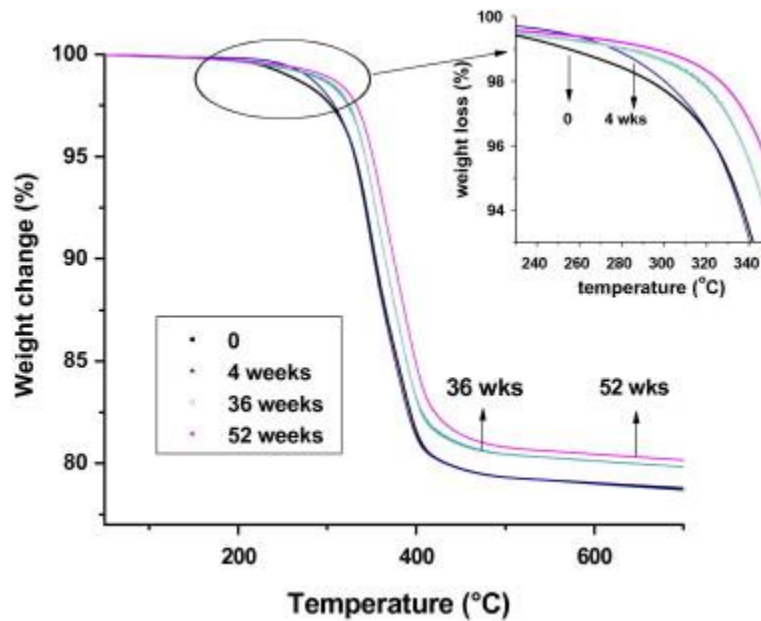


Fig. 10. TGA data for filled composite samples pre-aged in 200 °C air for 0, 4, 36, and 52 weeks. (For interpretation of the references to color in this figure legend, the reader is referred to the web version of this article.)

3.6 Thermal and mechanical properties

Prolonged aging effects are often manifest by changes in the T_g and the SBS strength. In contrast, fiber-dominated mechanical properties, particularly for unidirectional composites, are essentially unchanged even after long-term exposure, barring degradation of large portions of the matrix [18]. This study focused on changes in the SBS strength and the T_g , associated with matrix degradation with increasing aging time.



3.6.1 Glass-transition temperature (T_g)

Fig. 11 shows the T_g change of filled and unfilled-composite rods as a function of aging times up to 52 weeks. The T_g values for composite rods aged at 200 °C increased with aging time up to 12 weeks, then decreased from 12 to 36 weeks and remained nearly constant for the remainder of the exposure time. In addition, the T_g values for 36 and 52 weeks of exposure were less than those for un-aged composites. Aging at 180 °C caused the T_g values to also increase with increasing aging time, but at a slower rate compared to 200 °C aging. The T_g values continued to increase for aging times up to 36 weeks, then decreased slightly at 52 weeks, never falling below the initial T_g value. A similar trend was observed for T_g values of un-filled composite rods, as shown in Fig. 11.

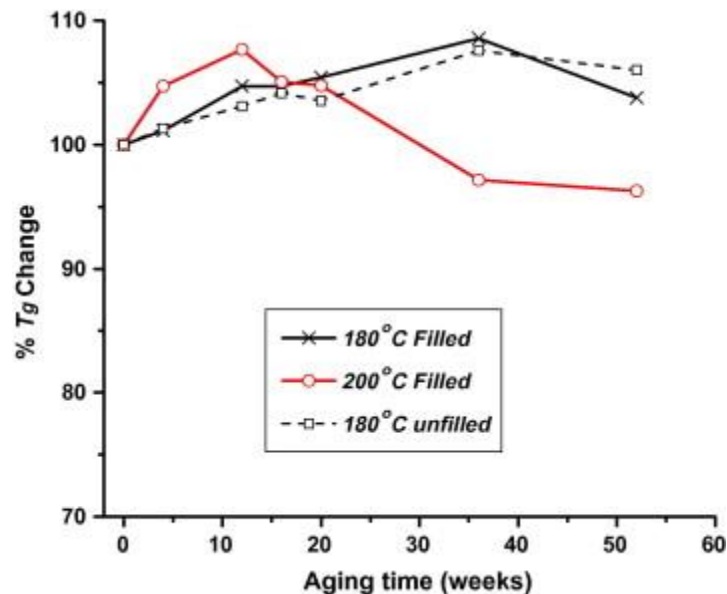


Fig. 11. Percent T_g change of filled and unfilled composite rods exposed in 180 °C and 200 °C air up to 52 weeks (8,736 h). (For interpretation of the references to color in this figure legend, the reader is referred to the web version of this article.)



The observed changes in T_g were attributed to the combined effects of post-crosslinking and thermal degradation (chain scission). Note that crosslinking reactions during isothermal exposure (such as post-curing reactions) generally include reactions between two (or more) active sites (e.g., $A + B \rightarrow X$, where A and B can be epoxy anhydride, carboxyle, etc.). The glass-transition temperature is directly proportional to the matrix crosslink density, $T_g = K_1 \log K_2 \alpha$, where α is the crosslink density, and K_1 and K_2 are the constants for a specific group of resins [22]. During aging, post-crosslinking reactions increased the number of crosslinks, decreasing molecular mobility and free volume, and increasing T_g . The crosslink density can be calculated approximately from DMA data using basic elasticity theory ($\nu_e = E'/3RT$), where ν_e is the crosslink density, E' is the storage modulus in the rubbery state, and R is the universal constant [23], as shown below.

Table 4 shows the crosslink densities for the composite matrix after aging at 180 °C for a range of aging times. The crosslink density increased monotonically for aging times up to 36 weeks, after which there was a slight decrease at 52 weeks. A similar trend was observed in T_g values measured for samples aged at 200 °C (see Fig. 11). The decreases in crosslink density and T_g that occur after long-term aging is commonly attributed to chain scission [24], a phenomenon that results in increased molecular mobility. Note oxidation had a negligible effect on the T_g change because the oxidation was superficial in nature, and DMA samples were sectioned from unoxidized core regions.



Table 4. Crosslink densities of composite matrix exposed at 180 °C for several aging time up to 1 year.

Aging time (weeks)	0	12	16	20	36	52
Crosslink density (kmol/m ³)	5025.6 ± 207.2	5931.0 ± 197.0	6636.3 ± 175.1	7130.1 ± 112.8	7970.9 ± 231.6	7746.1 ± 209.0

Composite samples were typically slightly under-cured because during pultrusion, the rod is formed and cured rapidly in just minutes. Consequently, a post-curing (post-crosslinking) reaction occurred during isothermal aging, continuing for up to 12 and 36 weeks at 200 °C and 180 °C, respectively. Eventually, the post-curing reaction stopped due to depletion of un-reacted epoxy groups. During post-curing, thermal degradation (via chain scission) occurred concurrently, albeit more slowly compared to post-curing. After reaching the maximum T_g value (after 12 weeks at 200 °C and 36 weeks at 180 °C), thermal degradation continued while post-curing ceased. The cessation of post-curing occurred at 12 weeks for exposure at 200 °C (compared to 36 weeks at 180 °C), and this was attributed to an increase in the post-curing reaction rate (Arrhenius law). Similarly the degradation reaction rate increased with increasing exposure temperature (Fig. 11), resulting in a more rapid decrease in T_g . In this case, the matrix degradation rate at 180 °C for up to 1 year was negligible compared to the rate at 200 °C.

3.6.2 Shear properties (strength and modulus are presented)

Long-term thermal exposure caused changes in the short beam shear (SBS) strength of the composite rods. Fig. 12a shows the SBS strength as a function of exposure time for filled composite rods aged at 180 °C and 200 °C, while Fig. 12b shows the SBS strength change for filled and unfilled rods



exposed at 200 °C up to 52 weeks. The values of SBS strength decreased with exposure time, reflecting chemical changes in the matrix during aging. Thermal aging resulted in matrix embrittlement, allowing fracture to occur at lower stresses [9].

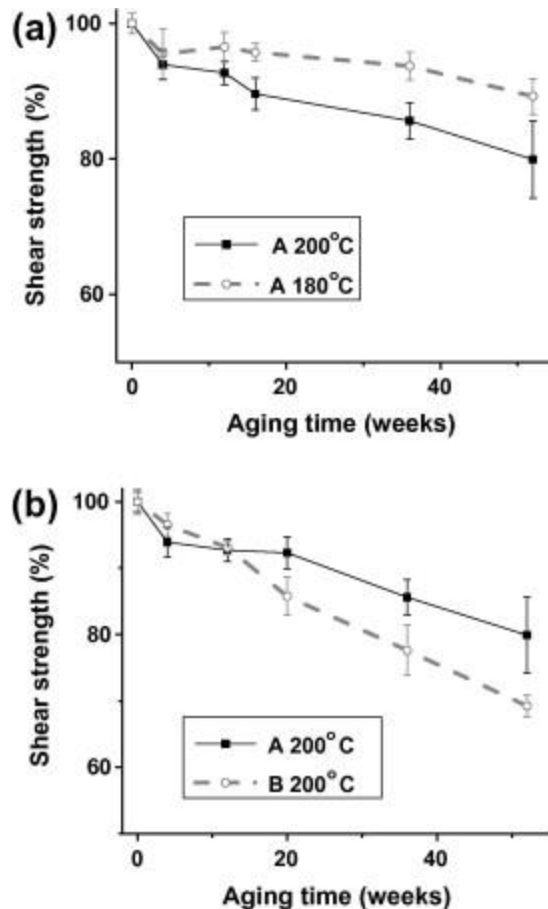


Fig. 12. (a) Percent change in SBS strength of the filled composite rods aged at 180 °C and 200 °C for 52 weeks (1 year) and (b) % change in SBS strength of the filled and unfilled composite rods aged at 200 °C for 52 weeks (1 year).

Fig. 12a shows a decrease of almost 10% in SBS strength for samples aged at 180 °C for 1 year. The SBS strength decreased by nearly 5% from 36 to 52 weeks. During this period, T_g values decreased as well, due to the cessation of crosslinking at 36 weeks of exposure, after which the degradation



reaction was the primary mechanism. The SBS strength decreased more rapidly with aging time at 200 °C, decreasing ~20% after 52 weeks (compared to a ~10% decrease at 180 °C). Note that over the aging period of 12–52 weeks at 200 °C, the SBS strength decreased ~15%, much like the decrease in T_g values (shown in Fig. 11). Thus, even at temperatures below the matrix T_g , increasing the aging temperature increased the degradation rate of the composite, thus accelerating the decrease in SBS.

Fig. 12b shows the change in SBS strength for filled (A) and unfilled (B) composite rods with aging times up to 52 weeks at 200 °C. The SBS decreased ~30% for unfilled rods after 52 weeks of exposure at 200 °C, while the decrease was ~20% for filled rods. Matrix cracks initiated and propagated within the near-surface regions of unfilled and filled rods, causing the decrease in SBS strength [24] and [25]. However, the cracking was more extensive in the unfilled rods, leading the greater and more rapid loss in SBS (Fig. 12b).

4. Conclusions

Oxygen-concentration profiles and the TOL values were determined for isothermally oxidized filled composites by applying a reaction-diffusion model. The model-based calculations of the TOL values were consistent with experimentally measured values (>90% accuracy). The predicted and measured TOL values for filled composites were slightly less than those of unfilled composites. The addition of kaolin fillers did not affect the oxidation mechanism or the reaction rate of the epoxy matrix, although it did cause a slight decrease in the oxygen-transport properties (diffusivity and solubility



of oxygen). While higher filler contents can be expected to further decrease the oxygen diffusivity, they may also introduce voids and other defects, and such defects may actually increase oxygen diffusivity, thereby accelerating matrix oxidation.

Predicting the degradation of composite mechanical and physical properties resulting from long-term oxidation requires consideration of diffusion and reaction rates of oxygen within the polymer matrix, geometry of the structure and exposing surface, fiber orientations, and polymer thermolysis. Although a reaction-diffusion model is appropriate for predicting the oxidation of polymer composites during early stages of oxidation, the predicted oxygen-concentration profiles can deviate from the measured data in later stages primarily because of shrinkage-induced cracks, and secondarily because of chemical changes in the matrix that alter the diffusivity and the reaction-rate parameters within the oxidizing surface layer. Furthermore, sample shape and fiber orientations can significantly influence the progression of oxidation, inhibiting or even preventing the initiation and propagation of such cracks. In the present case, the absence of sample edges appears to significantly inhibit composite oxidation. During the oxidation of unidirectional rods, a passive surface layer ($\sim 100 \mu\text{m}$) develops over time, and the oxygen diffusivity asymptotically approaches zero within the TOL. As a result, oxidation gradually ceases, after which the reaction-diffusion model is no longer valid. After the oxidation stops, the primary mechanism of degradation changes from thermal oxidation to thermal degradation. The oxidized layer continues to act as a passive surface layer, protecting against further matrix oxidation. Polymer-matrix composites often undergo thermal degradation when exposed to oxidizing environments at temperatures approaching T_g , and the extent of degradation depends on the thermal stability of the polymer network. For the thermally aged

Please cite this article as E. Barjasteh, S. Nutt “**The effect of filler on thermal aging of next-generation power lines**”, *Composites A*, 42 [12] 1873-1882 (2011)
DOI<<http://dx.doi.org/10.1016/j.compositesa.2011.08.006>>



composite rods in the present study ($T_g \sim 225\text{ }^\circ\text{C}$), matrix degradation occurred during an exposure for 1 year at $200\text{ }^\circ\text{C}$, while the extent of degradation (as measured by gravimetric experiments) at $180\text{ }^\circ\text{C}$ was much less. Matrix degradation was manifest in reductions in matrix-dominated properties, including SBS strength and T_g . Thus, the maximum long-term service temperature for rods with high T_g values will depend largely on the thermal stability of the polymer network (more than on the T_g value). Note that although the composite degradation after a year of aging was most evident in the matrix-dominated mechanical properties (particularly the SBS strength), the effect on fiber-dominated mechanical properties (such as tensile strength) was negligible.

Acknowledgements: Financial support from Composite Technology Corporation is gratefully acknowledged.

References:

1. A. Alawar, J. Bosze E, R. Nutt S, *A composite core conductor for low sag at high temperatures*, IEEE Trans Power Delivery (2005), p. 20
2. E.J. Bosze, A. Alwar, O. Bertschger, Y. Tsai, S.R. Nutt, *High-temperature strength and storage modulus in unidirectional hybrid composites*, Compos Sci Technol, 66 (2006), pp. 1963–1969
3. R. Boukehili, H. Ben Daly, A. Gasmi, *Physical and mechanical properties of pultruded composites containing fillers and low profile additives*, Polym Compos, 27 (2006), pp. 71–73
4. Lackey E, Vaughan JG, Washabaugh F, Usifer D, Ubrich P. Effects of fillers on pultrusion processing and pultruded properties. In: International composites EXPO '99 proceedings – composites institute 1999;21 E:1-10.
5. Vaughan JG, Lackey E. If you want high performance from your pultruded composites, pay attention to the filler. Technical papers – CFA composites 2000. CDROM; 2000.
6. E. Barjasteh, E.J. Bosze, S.R. Nutt, *Thermal oxidation of anhydride cured epoxy and epoxy matrix composites*, SAMPE Proc, 52 (2008), p. 12
7. V. Bellenger, J. Decelle, N. Huet, *Aging of a carbon epoxy composite for aeronautic applications*, Composites: Part B, 36 (2005), pp. 189–194

Please cite this article as E. Barjasteh, S. Nutt “**The effect of filler on thermal aging of next-generation power lines**”, Composites A, 42 [12] 1873-1882 (2011)
DOI<<http://dx.doi.org/10.1016/j.compositesa.2011.08.006>>



8. G.P. Tandon, K.V. Pochiraju, G.A. Schoepner, *Modeling of oxidative development in PMR-15 resin*, *Polym Degrad Stab*, 91 (2006), pp. 1861–1869
9. T.K. Tsotsis, S.M. Lee, *Long-term thermo-oxidative aging in composite materials: failure mechanisms*, *Compos Sci Technol*, 58 (1998), pp. 355–368
10. K.J. Bowles, M. Madhukar, D.S. Papadopoulos, L. Inghram, L. McCorkle, *The effects of fiber surface modification and thermal aging on composite toughness and its measurement*, *J Compos Mater*, 31 (6) (1997), pp. 552–579
11. X. Colin, A. Mavel, C. Marais, J. Verdu, *Interaction between cracking and oxidation in organic matrix composites*, *J Compos Mater*, 39 (2005), pp. 1371–1389
12. I.M. Salin, J.C. Seferis, *Anisotropic effects in thermogravimetry of polymeric composites*, *J Polym Sci*, 31 (1993), pp. 1019–1027
13. E. Barjasteh, E.J. Bosze, Y.I. Tsai, S.R. Nutt, *Thermal aging of fiberglass/carbon-fiber hybrid composites*, *Compo Part A: Appl Sci Manuf*, 40 (12) (2009), pp. 2038–2045
14. X. Colin, J. Verdu, *Strategy for studying thermal oxidation of organic matrix composites*, *Compos Sci Technol*, 65 (2005), pp. 411–419
15. H.M. Le Huy, V. Bellenger, M. Paris, J. Verdu, *Thermal oxidation of anhydride cured epoxies III. Effect on mechanical properties*, *Polym Degrad Stab*, 41 (1993), pp. 149–156
16. R. Yang, Y. Ling, J. Yu, K. Wang, *Thermal oxidation products and kinetics of polyethylene composites*, *Polym Degrad Stab*, 91 (2006), pp. 1651–1657
17. K.D. Ziegel, H.K. Frensdorff, D.E. Blair, *Measurement of hydrogen isotope transport in poly-(vinyl fluoride) films by the permeation-rate method*, *J Polym Sci: Part A-2*, 7 (1969), pp. 809–819
18. T.K. Tsotsis, *Thermo-oxidative aging of composite materials*, *J Compos Mater*, 29 (1995), pp. 410–422
19. R.N. Rethon, *Particulate-filled polymer composites*, Longman, Harlow (2003) p. 450
20. A.J. Kinloch, A.C. Taylor, *Mechanical and fracture properties of epoxy/inorganic micro- and nano-composites*, *J Mater Sci Lett*, 22 (2003), pp. 1439–1441
21. J. Tark Han, K. Cho, *Layered silicate-induced enhancement of fracture toughness of epoxy modeling compounds over a wide temperature range*, *Macromol Mater Eng*, 290 (2005), pp. 1184–1191
22. J. Unsworth, Y. Li, *Thermal degradation of epoxy/silica composites monitored via dynamic mechanical thermal analysis*, *J Appl Polym Sci*, 46 (1992), pp. 1375–1379

Please cite this article as E. Barjasteh, S. Nutt “**The effect of filler on thermal aging of next-generation power lines**”, *Composites A*, 42 [12] 1873-1882 (2011)

DOI<<http://dx.doi.org/10.1016/j.compositesa.2011.08.006>>



23. W.J. Cantwell, A.C. Roulin-Moloney, *Fractography and failure mechanisms of unfilled and particulate filled epoxy resins*, *Fractogr Fail Mech Polym Compos* (1989), pp. 233–290
24. D. Leveque, A. Schieffer, A. Mavel, J.F. Maire, *Analysis of how thermal aging affects the long-term mechanical behavior and strength of polymer–matrix composites*, *Compos Sci Technol*, 65 (2005), pp. 395–401
25. M.R. Winsom, *Modelling the effect of cracks on interlaminar shear strength*, *J Compo - Part A: Appl Sci Manuf*, 27 (1996), pp. 17–24